Nonclassic Functions of Human Topoisomerase I: Genome-Wide and Pharmacologic Analyses

Ze-Hong Miao,[1] Audrey Player,[2] Uma Shankavaram,[1] Yong-Hong Wang,[2] Drazen B. Zimonjic,[3] Philip L. Lorenzi,[1] Zhi-Yong Liao,[1] Hong Liu,[5] Tsutomu Shimura,[1] Hong-Liang Zhang,[1] Ling-Hua Meng,[1] Yong-Wei Zhang,[1] Ernest S. Kawasaki,[2] Nicholas C. Popescu,[3] Mirit I. Aladjem,[1] David J. Goldstein,[4] John N. Weinstein,[1] and Yves Pommier[1]

Laboratories of [1]Molecular Pharmacology and [2]Experimental Carcinogenesis, [3]Office of Science and Technology Partnerships, Center for Cancer Research, [4]Microarray Facility, Advanced Technology Center, National Cancer Institute, and [5]Clinical Endocrinology Branch, National Institute of Diabetes and Digestive and Kidney Diseases, NIH, Bethesda, Maryland

Abstract

The biological functions of nuclear topoisomerase I (Top1) have been difficult to study because knocking out *TOP1* is lethal in metazoans. To reveal the functions of human Top1, we have generated stable Top1 small interfering RNA (siRNA) cell lines from colon and breast carcinomas (HCT116-siTop1 and MCF-7-siTop1, respectively). In those clones, Top1 is reduced ~5-fold and Top2α compensates for Top1 deficiency. A prominent feature of the siTop1 cells is genomic instability, with chromosomal aberrations and histone γ-H2AX foci associated with replication defects. siTop1 cells also show rDNA and nucleolar alterations and increased nuclear volume. Genome-wide transcription profiling revealed 55 genes with consistent changes in siTop1 cells. Among them, asparagine synthetase (ASNS) expression was reduced in siTop1 cells and in cells with transient Top1 down-regulation. Conversely, Top1 complementation increased ASNS, indicating a causal link between Top1 and ASNS expression. Correspondingly, pharmacologic profiling showed L-asparaginase hypersensitivity in the siTop1 cells. Resistance to camptothecin, indenoisoquinoline, aphidicolin, hydroxyurea, and staurosporine and hypersensitivity to etoposide and actinomycin D show that Top1, in addition to being the target of camptothecins, also regulates DNA replication, rDNA stability, and apoptosis. Overall, our studies show the pleiotropic nature of human Top1 activities. In addition to its classic DNA nicking-closing functions, Top1 plays critical nonclassic roles in genomic stability, gene-specific transcription, and response to various anticancer agents. The reported cell lines and approaches described in this article provide new tools to perform detailed functional analyses related to Top1 function. [Cancer Res 2007;67(18):8752–61]

Introduction

DNA topoisomerase I (Top1) is biologically and pharmacologically important for at least two reasons related to what might be considered its classic activity, enzymatic DNA nicking-closing. First, it is essential for the removal of topological stress in DNA associated with replication, transcription, repair, and recombination (1, 2). Second, it is the sole molecular target of camptothecins, which are used to treat human cancers (3–5).

The essential nature of Top1 is reflected in the fact that animals [e.g., *Drosophila* (6) and mice (7)] whose *TOP1* gene is inactivated die at an early stage of embryogenesis. The survival of budding and fission yeasts without Top1 has been explained by compensation by topoisomerase II (Top2; ref. 2). The enzymatic function of Top1 avoids the accumulation of DNA supercoiling during replication and transcription (1, 2). Top1-mediated DNA cleavage-religation proceeds by the formation and resealing of covalent enzyme-DNA intermediates, which are referred to as the cleavage complexes (Top1cc). Top1cc form with broad sequence selectivity, allowing the enzyme to act at a large number of sites in the genome.

The natural alkaloid camptothecin and its therapeutic derivatives, topotecan and the active metabolite of irinotecan, selectively trap Top1cc by binding at the interface of the Top1-DNA cleavage complex (3, 5). Top1cc can also be stabilized by promiscuous endogenous DNA modifications (8) such as abasic sites, mismatches, and nicks and by carcinogenic adducts formed by benzo(*a*)pyrene diol epoxide, vinyl chloride, acetaldehyde, and 4-nitroquinoline-1-oxide (4NQO; refs. 8, 9). Such cleavage complexes are particularly damaging when they produce collisions with replication forks, thereby introducing DNA double-strand breaks that can be detected as histone γ-H2AX foci (10). Recently, we also found that Top1cc form early during apoptosis (5, 11).

Besides regulating DNA topology, Top1 has been proposed to serve other important functions that might be considered as independent of its classic DNA cleavage-religation activity. First, Top1 may directly interact with many host cell proteins, including DNA repair factors, transcription factors, RNA splicing factors, cell cycle regulators, apoptosis-related proteins, and viral proteins,[6] suggesting the involvement of Top1 in a variety of physiologic processes mediated by those factors. Second, Top1 may serve as a general transcription cofactor by binding to the core transcription initiation complex (transcription factor IID; refs. 12, 13) to regulate transcription (12, 14). Top1 has also been suggested to activate transcription of specific genes [including epidermal growth factor receptor (EGFR)] by binding to c-Jun (15). Finally, Top1 may also regulate transcription by acting as a specific protein kinase for SR proteins, thereby contributing to RNA splicing (16).

The evidence for many of those classic and especially nonclassic functions is fragmentary or indirect. Hence, we wished to establish

Note: Supplementary data for this article are available at Cancer Research Online (http://cancerres.aacrjournals.org/).

Requests for reprints: Yves Pommier, Laboratory of Molecular Pharmacology, Building 37, Room 5068, NIH, Bethesda, MD 20892-4255. Phone: 301-496-5944; Fax: 301-402-0752; E-mail: pommier@nih.gov.

doi:10.1158/0008-5472.CAN-06-4554

6 http://www.hprd.org/protein/00535?selectedtab=INTERACTIONS

an experimental system with which to examine the possible functions of vertebrate Top1 in as well controlled a way as possible. Accordingly, we have generated and characterized colon and breast carcinoma cell lines stably transfected with small interfering RNA (siRNA) to down-regulate Top1.

Materials and Methods

Cell culture and establishment of stable siTop1 cell lines. HCT116 (NCI-DTP), MCF-7 (American Type Culture Collection), and the derived siTop1 and siCtrl cell lines were grown in DMEM plus 10% (vol/vol) heat-inactivated FCS.

The genetic constructs for the Top1-knockdown cell lines are detailed in Supplementary Fig. S1. Hygromycin B–resistant clones were selected, and the resulting cell lines were designated as HCT116-siTop1, MCF-7-siTop1, HCT116-siCtrl, and MCF-7-siCtrl. The doubling times of the siTop1 and siCtrl cell lines was comparable.

Drug effects were assessed by sulforhodamine B (SRB) assays (Sigma-Aldrich; ref. 9).

Western blotting. Top1 monoclonal antibody was a kind gift from Dr. Yung-Chi Cheng (Yale University, New Haven, CT). Top2α and Top2β antibodies were from Abcam Inc. and BD, respectively. Top3α and Top3β antibodies were from Santa Cruz Biotechnology, Inc. Western blotting was done using electrochemiluminescent reagents (Pierce) and high-performance Hyperfilm-ECL (Amersham Biosciences).

Cleavage complexes were detected by the immunocomplex of enzyme (ICE) bioassay (9, 11).

Cytogenetic analyses and NOR staining. Spectral karyotyping (SKY) analyses were done as described (17). For NOR staining (18), chromosome spreads were stained, and metaphases were digitally recorded in two separate channels: fluorescent 4′,6-diamidino-2-phenylindole (DAPI) to visualize chromosomes and transmitted light to record silver grains. Those gray-scale images were adjusted for contrast, inverted, merged, and pseudo-colored.

Micrococcal nuclease digestions. Nuclei were extracted using the TransFactor Extraction Kit (BD Biosciences) and digested with 1 unit/mL micrococcal nuclease (Sigma-Aldrich Co.) under standard conditions. DNA was purified and resolved by 1% agarose gel electrophoresis.

Immunofluorescence microscopy. Cells were lysed in hypotonic buffer [10 mmol/L Tris-HCl (pH 7.4), 2.5 mmol/L $MgCl_2$, 1 mmol/L phenylmethylsulfonyl fluoride, and 0.5% Nonidet P-40]. After being fixed, permeabilized, and blocked, cells were reacted with antibodies against proliferating cell nuclear antigen (PCNA; Santa Cruz Biotechnology) and γ-H2AX (Upstate Technology). Slides were incubated with secondary antibodies conjugated with Alexa-488 or Cy-3 and counterstained for DNA with DAPI. To observe nuclei and nucleoli, cells were stained with propidium iodide (PI). Images were captured by confocal microscopy (Nikon-PCM-2000).

Bromodeoxyuridine incorporation. Following 30 min pulse-labeling with 50 μmol/L bromodeoxyuridine (BrdUrd, Calbiochem), cells were collected and stained with FITC-conjugated anti-BrdUrd antibody (Becton Dickinson). Cells were resuspended in 500 μL PI solution (50 μg/mL PI and 50 μg/mL RNase) and analyzed with a FACScan flow cytometer (Becton Dickinson).

Oligo microarrays and data analyses. Total RNA was extracted (RNeasy-Midi-Kit, Qiagen) and stored at −80°C. Antisense RNA (aRNA) was generated using 1 μg total RNA (Ambion-Message-Amp2-aRNA kit, Ambion). Biotin-CTP (Enzo-Biochemicals) and biotin-UTP (Roche Molecular Biochemicals) were incorporated during *in vitro* transcription. Quality controls were determined by BioAnalyzer Nano6000 Assay (Agilent Technologies). About 15 μg each of biotin-labeled aRNA were fragmented and hybridized as technical replicates to U133-plus-2-Genechips (Affymetrix). Genechips microarrays were washed, stained, scanned and saved as CEL files.

CEL files were analyzed using programs developed in R, a programming language and developer environment for statistical computing and graphics.[7] The Robust Multi-array Analysis (RMA) algorithm as implemented in the BioConductor package was employed for data normalization using the quantile method.[8] This method aims at making the distribution of probe intensities the same across all arrays in a given set. Gene expression signal calculation was based on Perfect Match values from each probe set. To identify differentially expressed genes, RMA data were subjected to significance analysis of microarrays (SAM) with a false discovery rate (FDR) set to 5%.

Array comparative genomic hybridization analyses. Total DNA was analyzed in duplicate for comparative genomic hybridization (CGH; NimbleGen Systems). The data of all the probes against a given gene based on its chromosome location were extracted and averaged to determine the change in gene copy in the siTop1 cells relative to the corresponding siCtrl cells.

Top1 complementation in the siTop1 cells. Top1 cDNA was inserted into the mammalian expression vector pcDNA3.1/V5-His-TOPO (Invitrogen) to generate the pV5-Top1. For Top1 complementation, we mutated the Top1 DNA sequence in pV5-Top1 to eliminate the Top1-siRNA targeting sequence while preserving the amino acid code. Those silence mutations were introduced in the pV5-Top1 vector using the QuickChange site-directed mutagenesis kit (Stratagene) with the primers 5′-CTCATGGAGGGCCTGACCGCTAAGGTGTTCCGTACGTAC-3′ (forward) and 3′-GAGTACCTCCCGGACTGGCGATTCCACAAGGCATGCATG-5′ (reverse; s MWG-Biotech Inc.; Fig. 5*C*). The silent-mutated pV5-Top1, designated as pV5-Top1-sm, was transfected into the siTop1 cells. Asparagine synthetase (ASNS) mRNA was detected using Quantigene Branched-DNA Assays (Genospectra Inc.). The ASNS mRNA level for a given sample was then normalized to the cyclophilin B level for that sample.

Acute transfection with siRNAs against Top1 and ASNS. Two Top1 siRNAs (Top1-1 and Top1-2, respectively) targeting the Top1 cDNA sequences were generated: 5′-AAGTGGAAATGGTGGGAAGAA-3′ and 5′-AAGGACTCCATCAGATACTAT-3′ (Qiagen). The control siRNA random sequence was 5′-UCCAGUGAAUCCUUGAGGUdTdT-3′. The siASNS sequence consisted of sense r(GGAUACUGCCAAUAAGAAA)dTdT and antisense r(UUUCUUAUUGGCAGUAUCC)dAdG, designed against the target CTGGATACTGCCAATAAGAAA (exon 5, nt 556). Cells were transfected with the siRNAs with Oligofectamine transfection reagent (Invitrogen).

Results

Topoisomerase activities in the siTop1 cell lines. The main steps used to produce the shRNA vectors and siRNA cell lines are described in Supplementary Fig. S1. Cell pairs (siTop1 and siCtrl) were generated by transfection of the construct into human colon carcinoma HCT116 and breast carcinoma MCF-7 cells, followed by selection for resistance to hygromycin B.

When examined by Western blotting, all of the siTop1 clones expressed Top1, albeit at much reduced levels. Two of the clones were selected for further studies based on their consistently low Top1 expression. Top1 protein levels were 10% to 20% of that in their respective control cell lines (Fig. 1*A*). Top1 down-regulation has been stable for more than 3 months in hygromycin B–free medium, indicating the effectiveness and stability of Top1 knockdown. Western blotting also showed no significant change in global protein levels for Top2α, Top2β, Top3α, or Top3β (Fig. 1*B*).

To determine whether Top1 down-regulation was accompanied by concurrent changes in topoisomerase activity at the chromatin level, we used camptothecin to trap Top1cc and then detected Top1 bound to cellular DNA by immunoblot following cesium gradient centrifugation (Fig. 1*C*; refs. 9, 19, 20). Both siTop1 cell

[7] http://www.r-project.org
[8] http://bioconductor.org

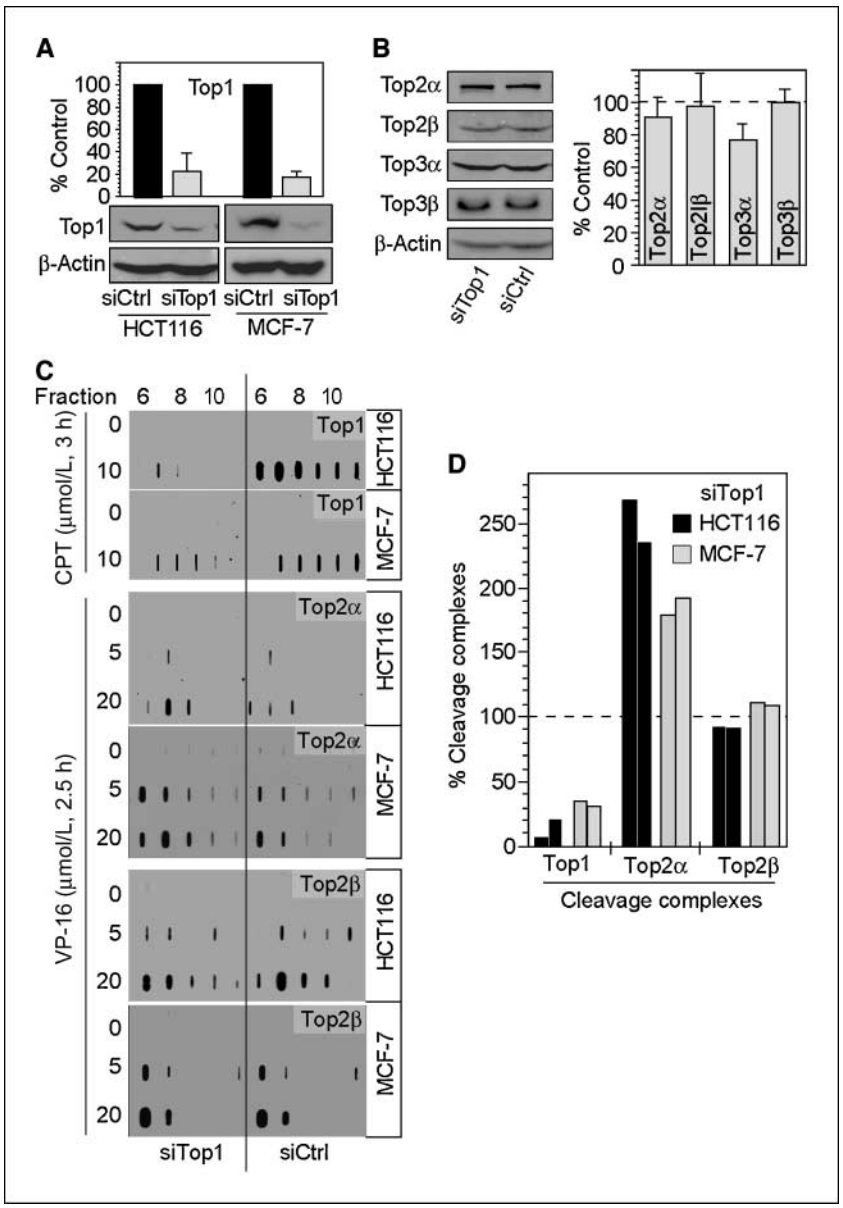

Figure 1. Topoisomerase expression and topoisomerase cleavage complexes in the siTop1 cell lines. *A,* total cellular Top1 protein levels were detected by Western blotting in HCT116- and MCF-7–derived cells. Quantitation was conducted with Adobe Photoshop 7.0, and the relative Top1 protein levels are expressed as mean ± SD, $n = 3$. *B,* total protein levels for Top2α, Top2β, Top3α, and Top3β were detected and quantified as in (*A*). *C,* chromatin-associated Top1 was evaluated as cleavage complexes in camptothecin (*CPT*)-treated cells using the ICE-bioassay. Fractions collected from the cesium chloride gradients are indicated above the immunoblot. Chromatin-associated topoisomerases II (*Top2α* and *Top2β*) were evaluated as cleavage complexes in etoposide (*VP-16*)–treated cells using the ICE-bioassay. *D,* quantitation of Top1, Top2α, and Top2β associated with chromatin. Data are from ICE bioassay experiments with 10 μmol/L CPT for Top1 and 20 μmol/L VP-16 for Top2α and Top2β as in (*B* and *D*), and computed with Adobe Photoshop 7.0. The data show two representative independent experiments.

lines showed reduced trapping of Top1cc (Fig. 1*C* and *D*). Thus, Top1 down-regulation was effective at the chromatin level. Next, we determined whether chromatin-bound Top2 was changed in the siTop1 cell lines. For those studies, we used etoposide (VP-16), a specific Top2 inhibitor. Both of the siTop1 cell lines formed significantly more Top2α cleavage complexes (Fig. 1*C* and *D*). In contrast, Top2β cleavage complexes were unchanged in the Top1–down-regulated cell lines (Fig. 1*C* and *D*). Because etoposide targets both Top2α and Top2β, those experiments indicate a selective increase in the association of Top2α with chromatin in the Top1–down-regulated cell lines and suggest that Top2α compensates for defective Top1 at the chromatin level.

High frequency of genomic reorganizations in Top1-deficient cell lines. MCF-7 cells are notorious for intrinsic genomic instability and fast acquisition of karyotypic differences in culture (21, 22). In contrast, HCT116 has a stable, near-diploid chromosome number with only four structural chromosome rearrangements (17, 23), making it an ideal model for evaluation of genomic instability. Therefore, to detect the impact of Top1 reduction on genomic stability, we used comprehensive SKY-based karyotypic comparison of the HCT116-siTop1 and HCT116-siCtrl lines. Thirty-two metaphases each from HCT116-siTop1 and HCT-siCtrl were randomly selected and submitted to spectral karyotyping. The basic karyotype in both cases was the same as reported previously (17) and is best described as: 45, X, der(10)t(10;16), der(16)t(8;16), der(18)t(17;18). The mean chromosome number was comparable in both cell lines (44.9 ± 0.8 for the siCtrl cells and 45.0 ± 1.8 for the siTop1 cells, $P = 0.348$). Detailed spectral karyotype analysis, however, revealed increased numerical aberrations in HCT116-siTop1. Thirty-two metaphases from the control cells showed altogether 12 numerical aberrations per pool of 1,436 chromosomes, whereas that value in HCT116-siTop1 cells was increased almost 3-fold to 32 per pool of 1,440 chromosomes ($P = 0.0193$). Much larger differences between the two cell lines were observed for structural aberrations. Thirty-two metaphases from control cells showed only one [t(10;14)] translocation, whereas corresponding

samples from HCT116-siTop1 cells showed 17 deletions, translocations, and inversions (P = 0.0002). When numerical and structural changes were pooled together, the statistical difference was highly significant (P = 0.0008; Fig. 2*A*). Those data indicate that Top1 knockdown is associated with genomic reorganizations in HCT116 cells.

Because ribosomal DNA (rDNA) alterations are among the most obvious phenotypes of Top1-deficient yeast (24), we used the controlled silver-staining assay to probe nucleolus organizing regions (NOR; ref. 18). NORs are comprised of rDNA sequences tandemly clustered on the short arms of the five acrocentric chromosomes (no. 13, 14, 15, 21, and 22). In both HCT116-siTop1 and -siCtrl, almost 100% of chromosomes 13, 15, and 22 were labeled, whereas chromosome 14 often showed only one labeled copy in both samples. The average number of NOR signals per acrocentric chromosome was smaller (0.79 $\pm$ 0.08) in HCT116-siTop1 cells compared with controls (0.86 $\pm$ 0.06), and this statistically significant ($P \leq 0.012$) difference may have resulted, in part, from the fact that in HCT116-siTop1, only one copy of chromosome 21 exhibited positive NORs, compared with HCT116-siCtrl cells where both copies were labeled (Fig. 2*B*) in nearly all metaphases (P = 0.0005). Those results suggest that Top1 deficiency may be associated with decreased NOR activity.

To evaluate whether Top1 down-regulation also affected chromatin structure, we used micrococcal assays. Figure 2*C* shows no detectable difference between HCT116 siCtrl and HCT116 siTop1 cells in the global distribution of nucleosomal arrays.

Top1 deficiency leads to the formation of histone γ-H2AX foci associated with replication. To find factors that contribute to the chromosomal changes observed in the siTop1 cells, we searched for histone γ-H2AX foci, which are indicators of genomic instability and DNA double-strand breaks (DSB; refs. 25, 26). Figure 3*A* and *B* shows that both HCT116- and MCF-7-siTop1 cell lines formed more endogenous γ-H2AX foci than did their respective control cell lines. Notably, those γ-H2AX foci were produced selectively in PCNA-positive cells (Fig. 3*A*), showing their association with DNA replication (10). Moreover, the γ-H2AX foci colocalized with the PCNA foci (Fig. 3*B*).

To examine replication, BrdUrd pulse-labeling experiments were done. They showed an overall reduction of BrdUrd incorporation in both the HCT116-siTop1 and MCF-7-siTop1 cells (24% and 29% reduction for HCT116-siTop1 and MCF-7-siTop1 compared with the corresponding siCtrl cells, respectively; Fig. 3*C*). Altogether, the γ-H2AX, PCNA, and BrdUrd data show that Top1 deficiency produces replication defects and replication-associated DSB (10).

Nuclear abnormalities in siTop1 cells. Figure 3*D* shows representative images of nuclei from the HCT116 and MCF-7 pairs. The size of the nuclei and number of nucleoli were greater in the Top1 siRNA cells than in the corresponding controls. The MCF-7-siTop1 showed the largest nuclei (Fig. 3*D, bottom*). Nucleolar structures were better separated from each other in MCF-7 than in HCT116, and the MCF-7-siTop1 showed clear increased number of nucleoli and heterogeneity in size. The

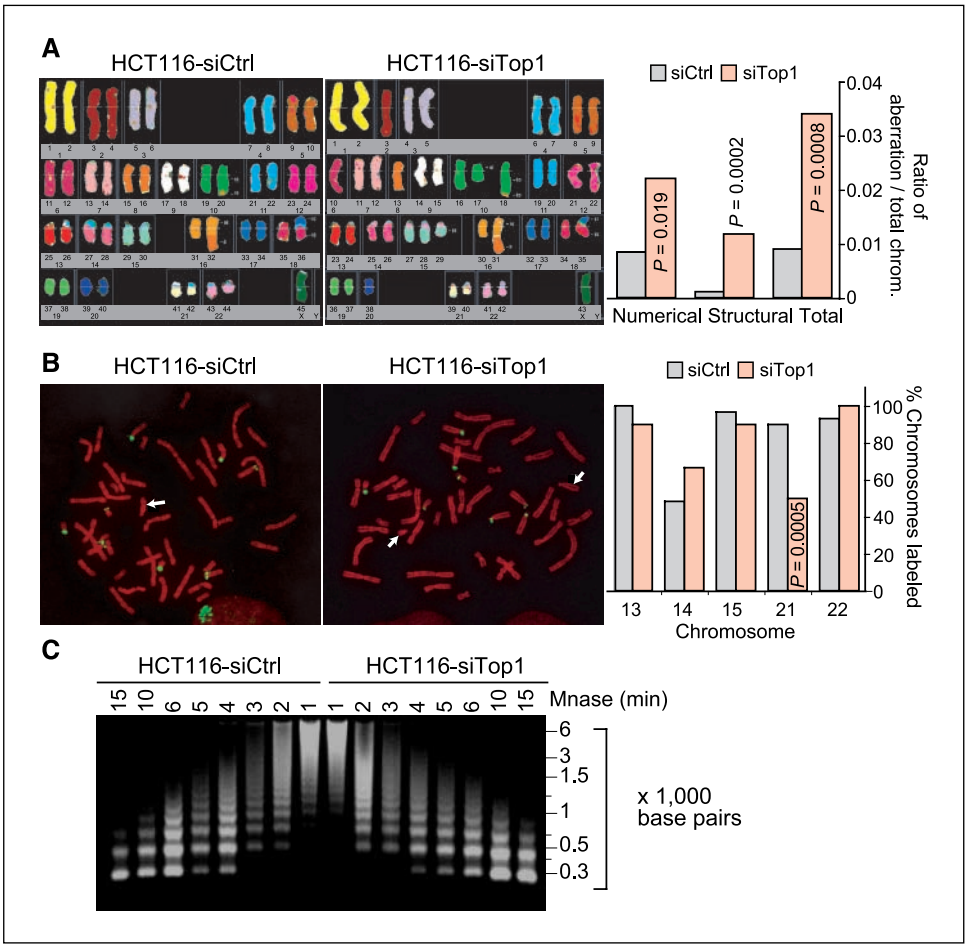

Figure 2. Chromosomal abnormalities in siTop1 cells. *A,* numerical, structural, and total chromosomal aberrations in HCT116-siTop1 cells. Representative karyotypes detected by SKY are shown. Chromosomal aberrations were computed from 32 metaphases for each cell line (*right*). *B,* staining of nucleolar organizing regions (*NOR*) in representative mitotic spreads shows nine signals in HCT116-siCtrl cells and eight in HCT116-siTop1 cells. *White arrows,* unlabeled acrocentric chromosomes. *Right,* overall distribution of signals per chromosome in both samples. *C,* global chromatin structure in HCT116-derived cells detected by digestion with 1 unit/mL micrococcal nuclease for the indicated times.

increased number of nucleoli was less in the HCT116-siTop1. Altogether, those observations suggest that Top1 deficiency affects nuclear and nucleolar structures.

Top1 selectively regulates gene transcription. To investigate a possible involvement of Top1 in the regulation of transcription, we studied mRNA levels using Affymetrix U133-plus-2-Genechips. The array contains 54,613 probe sets against more than 47,000 transcripts, including 17,942 different genes with HuGO (Human Genome Organization) names. A list of 308 candidate genes was generated by taking the changes common to two independent experiments on two different clones of the HCT116-derived sublines (Fig. 4*A*). The changes in mRNA levels of 19 genes chosen from that merged list were validated by quantitative reverse transcription-PCR (QRT-PCR; Supplementary Table S2). Western blotting also showed consistent changes for 14 of 15 genes assessed (Figs. 1*A* and 5*B* and Supplementary Fig. S2*A*). In addition, HCT116-siTop1 and HCT116-siCtrl cell lines showed similar mRNA half-lives (Supplementary Fig. S2*B*), excluding the possibility that differential mRNA degradation had led to the differences between the mRNA levels of those genes.

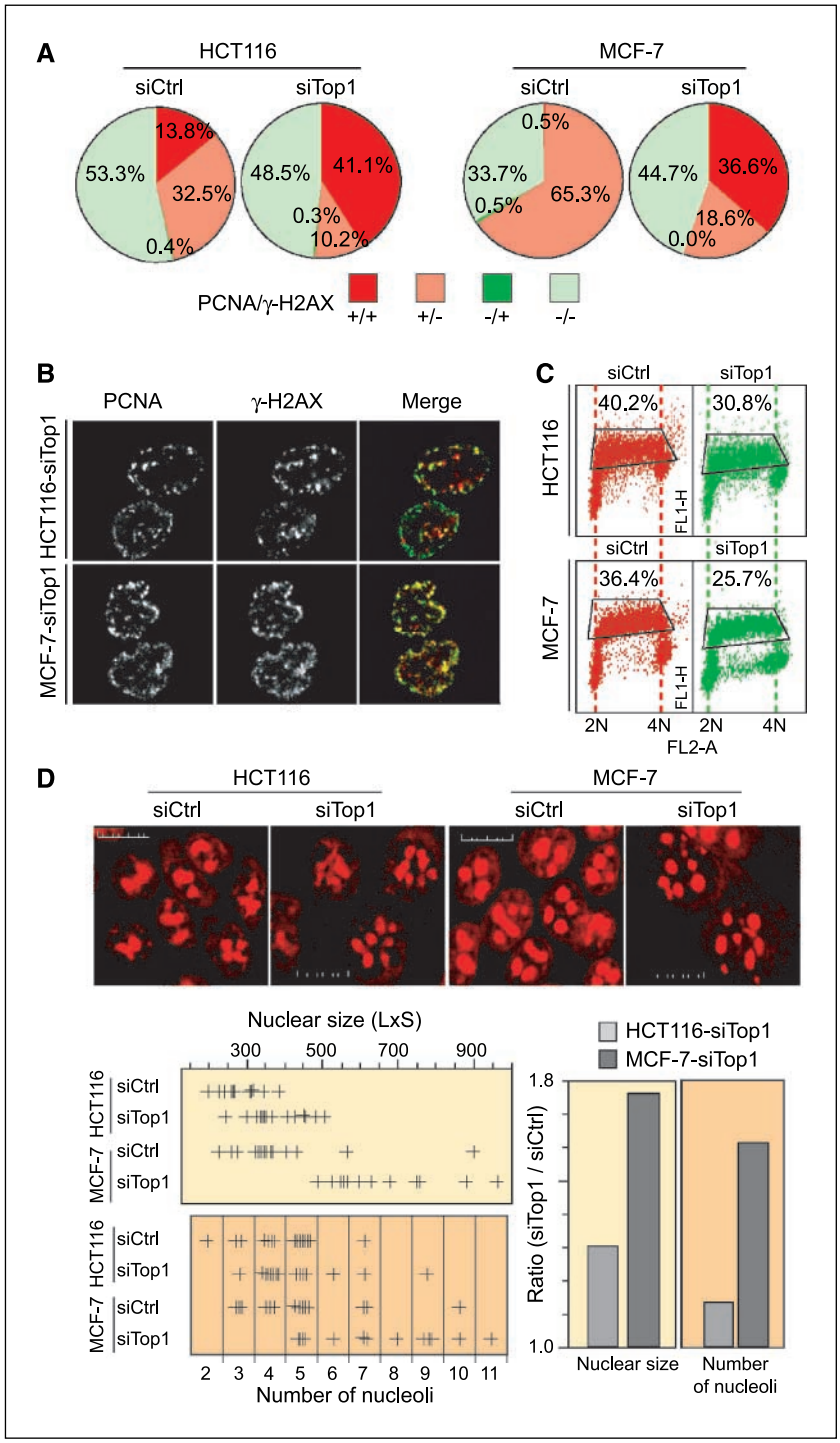

Figure 3. Increased γ-H2AX foci, reduced replication rate, increased nuclear size, and nucleolar number in the siTop1 cell lines. *A,* fractions of γ-H2AX–positive cells and PCNA-positive cells. About 400 cells were counted for each cell type. The color code is indicated below the pie charts. *B,* representative immunofluorescence images for γ-H2AX– and PCNA-positive siTop1 cells. *Green* and *red,* PCNA and γ-H2AX foci in the merged images, respectively. *Yellow foci,* colocalized signals. *C,* representative FACScan analyses following pulse-labeling with BrdUrd (30 min). BrdUrd and PI incorporation are plotted on the *Y*- and *X*-axes, respectively. Gated regions defined from the control cells without BrdUrd (data not shown) were used to calculate BrdUrd incorporation relative to total positive signal. Percentages are the mean of two independent determinations for % BrdUrd incorporation. *D, top,* representative images for nuclei and nucleoli after PI staining. *Bottom left,* quantitation of nuclear size and nucleoli numbers. Fifteen nuclei were chosen randomly and measured for each cell line. *Top,* nuclear size (approximated as the product of the long and short diameters of a given nucleus). *Bottom,* numbers of nucleoli per nucleus. *Bottom right,* relative increase in mean nuclear size and number of nucleoli in both siTop1 cell lines relative to the respective siCtrl cell lines. Data are the ratio of mean values obtained from the individual measurements derived from the analysis of 60 individual cells (*left*).

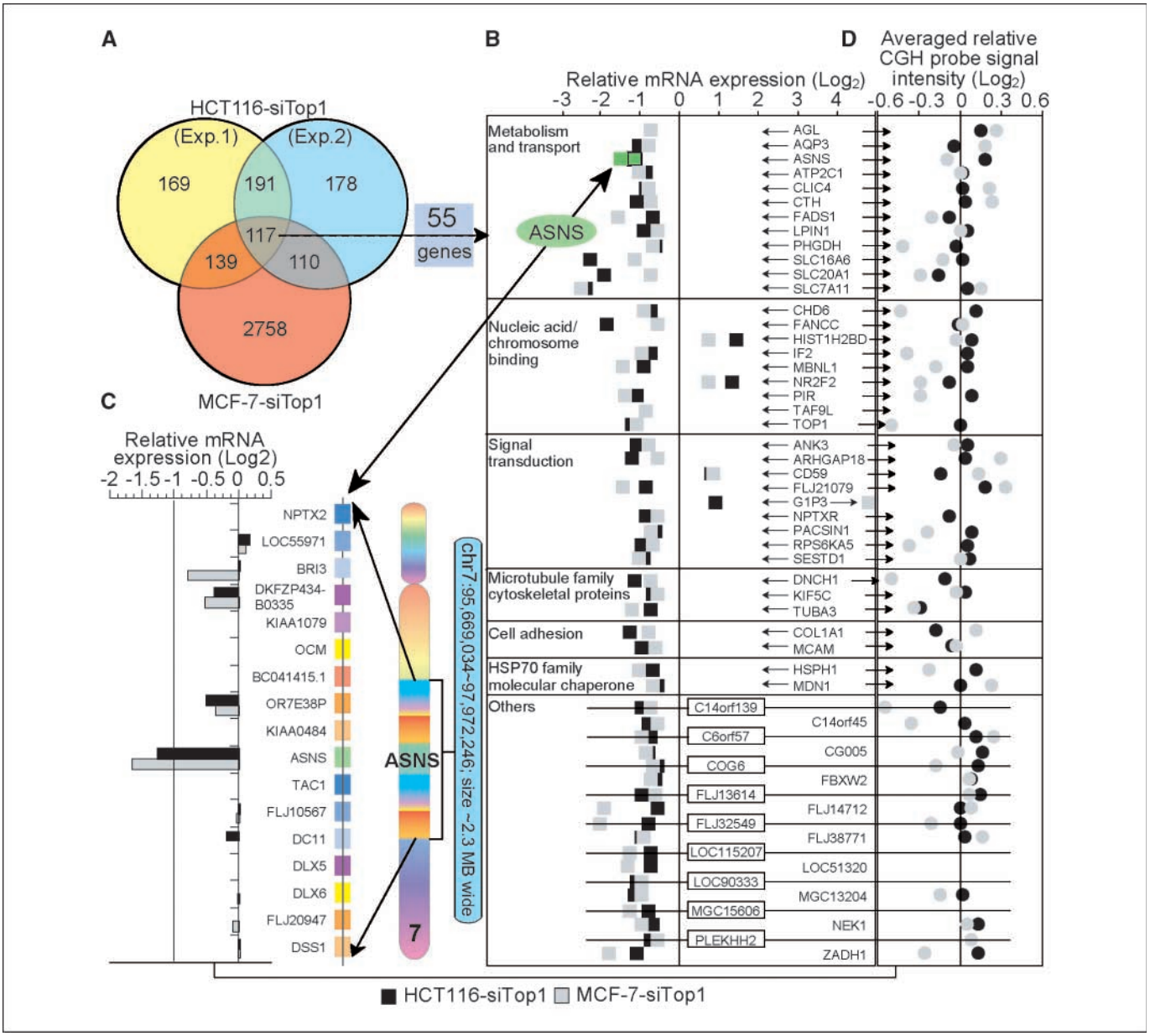

Figure 4. Selective transcription deregulation in the siTop1 cell lines. *A,* Venn diagrams showing the number of genes with significant changes in mRNA expression in three independent microarray experiments (*Exp.*). *Yellow* and *blue,* HCT116-siTop1 data. *Red,* MCF-7-siTop1 data. *B,* relative expression and functional classification of the 55 genes with consistent changes in mRNA level in both siTop1 cell lines. *Points,* means of eight values from two individual experiments for HCT116-siTop1 cells and the mean of four values from one experiment for MCF-7-siTop1 cells. *C,* relative expression of ASNS and of the genes flanking ASNS on chromosome 7. Data were collected from the microarray analyses. *D,* DNA copy numbers for the 55 genes with modified transcripts detected in the siTop1 cells. Analyses were done by array CGH. *Points,* averages of the data points of all the probes against the given gene in a duplicate experiment. In *B–D*, *black* and *gray,* HCT116-siTop1 and MCF-7-siTop1 cell lines, respectively.

To identify genes transcriptionally regulated by Top1, we did additional microarray analyses on the MCF-7-siTop1 and MCF-7-siCtrl cell lines. The data discussed in this publication have been deposited in the Gene Expression Omnibus[9] of the National Center for Biotechnology Information (NCBI) and are accessible through GEO series accession number GSE7161. Taking the genes differentially expressed in three separate experiments (one from the MCF-7–derived cell pair and the other two from replicates of the HCT116-derived pair) produced a list of 55 genes (Fig. 4*A* and *B* and Supplementary Table S1). Among those 55 genes, four were up-regulated (7.3%), and 51 were down-regulated (92.7%). Twelve of the genes are related to cellular substance metabolism and transport, nine genes to cellular signal transduction, and nine to nucleic acid or chromosome binding (Fig. 4*B* and Supplementary Table S1). Notably, expression of the genes coding for Top1-interacting proteins was not modulated in siTop1 cells at either the mRNA or protein level.

We next asked by CGH whether the mRNA changes observed in the Top1 siRNA cells were related to alterations in gene structure.

[9] http://www.ncbi.nlm.nih.gov/geo/

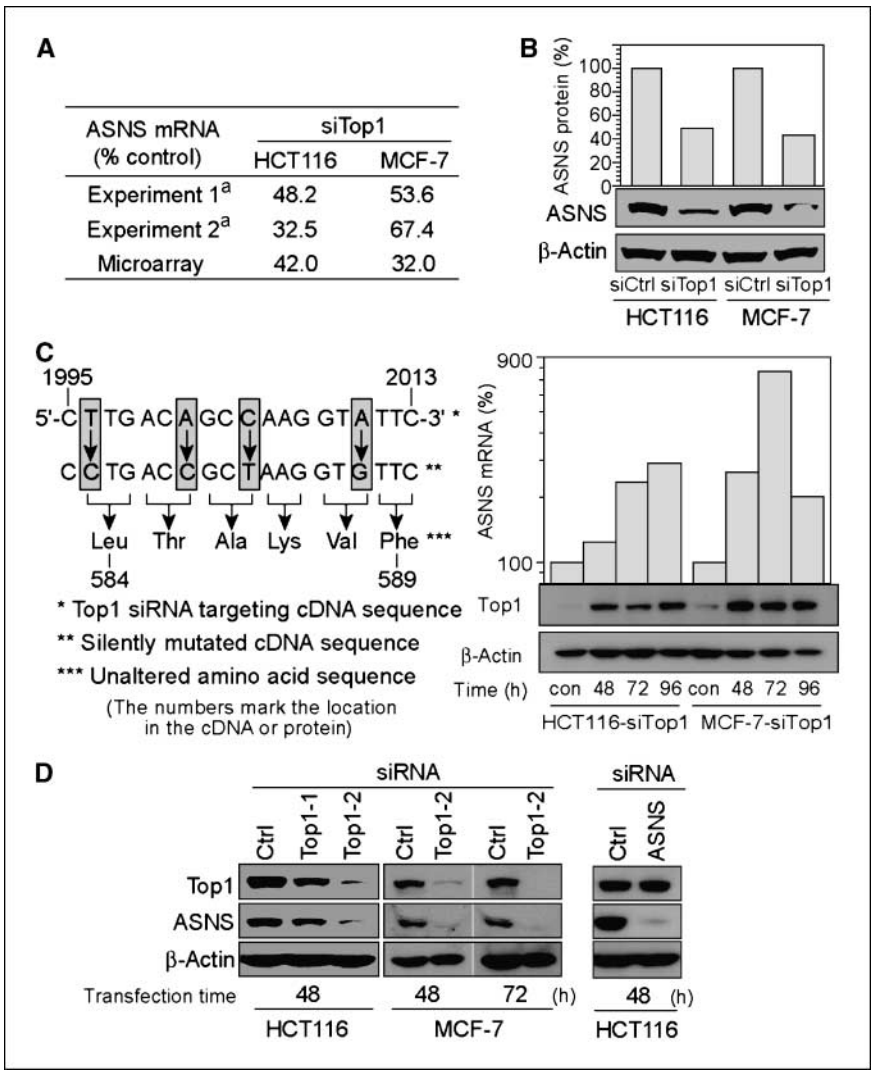

Figure 5. Top1 regulates the expression of the ASNS gene. *A,* levels of ASNS mRNA in the siTop1 cells relative to their respective siCtrl cells measured by Quantigene Branched-DNA assays (*superscript a*) or by microarray analyses. *B,* reduced ASNS protein levels in the siTop1 cells (average of two independent experiments giving consistent results in the bar graph; representative Western blot below). *C, left,* construct used for Top1 complementation. The Top1 cDNA sequence used to avoid siRNA targeting is shown. The corresponding plasmid is referred to as pV5-Top1-sm. *Right,* pV5-Top1-sm transfection effectively complements Top1 in the siTop1 cells and enhances ASNS expression. ASNS mRNA was measured by Quantigene Branched-DNA assays. Data are normalized to ASNS mRNA in the siTop1 control groups (*con,* not complemented; average of two independent experiments). *D,* down-regulation of ASNS protein in HCT116 or MCF-7 transiently transfected with two Top1 siRNAs of different sequences (Top1-1 and Top1-2) for 48 or 72 h. Transient transfection with ASNS siRNA does not change Top1 protein expression. Western blotting images are representative of at least two separate experiments.

Figure 4*D* shows only minor DNA copy number changes in the HCT116-siTop1 cells. Although the MCF-7-siTop1 showed more abnormalities, there was no correlation between genomic and mRNA alterations (compare in Fig. 4*B* and *D*), indicating that the gene dysregulation in siTop1 cells is due to transcription rather than genetic defects.

One of the transcripts down-regulated in the siTop1 cell lines was ASNS (Fig. 4*B, green ellipse*). To further analyze the relationship between ASNS and Top1, we measured mRNA levels of the genes within ~2.3 million bp of the ASNS gene (Fig. 4*C*). Among the 17 genes located in that region,[10] ASNS was the only one whose mRNA levels were changed by more than 50% in the siTop1 cells compared with their respective controls (Fig. 4*C*). Those results suggest that the down-regulation of ASNS in the siTop1 cells is not simply a regional genomic effect, and that the regulation of transcription by Top1 is gene specific.

Top1 regulates ASNS expression. The ASNS mRNA down-regulation observed by microarray analysis in the Top1 siRNA cell lines was confirmed independently using the Quantigene-Branched-DNA assay (Fig. 5*A*). Western blotting also showed reduced ASNS protein levels (Fig. 5*B*). To test the causal role of Top1 reduction in the decreased expression of the ASNS gene, we did Top1 complementation experiments. Because of the endogenously produced Top1 siRNA, we engineered a Top1 transfection vector (pV5-Top1-sm) with silent mutations in the Top1-siRNA target sequence (Fig. 5*C, left*). Transfection of pV5-Top1-sm effectively enhanced Top1 protein levels and also increased the expression of ASNS mRNA in a time-dependent manner in both HCT116-siTop1 and MCF-7-siTop1 cell lines (Fig. 5*C, right*), suggesting that Top1 plays a causal role in the regulation of ASNS expression, a conclusion further supported by the decreased expression of ASNS protein following transient transfection with Top1 siRNAs (Fig. 5*D*). Transfection of ASNS siRNA, on the other hand, had no effect on Top1 expression (Fig. 5*D, right*). Overall, those results indicate that Top1 positively regulates ASNS at the level of transcription.

Stable Top1 reduction changes drug responsiveness. Besides camptothecins, various DNA-interactive agents can trap Top1cc, including reactive oxygen species, alkylating agents, antimetabolites, and carcinogens (8, 9). Staurosporine also leads to the formation of apoptotic Top1cc (11). For many of those agents,

[10] http://genome.ucsc.edu

however, it has remained unclear whether and to what extent Top1cc contribute to the biological effects. We used the siTop1 cell lines to address that question. More than 20 compounds targeting at least 15 different molecular pathways, as well as ionizing and UV radiations, were investigated (Fig. 6 and Supplementary Tables S3 and S4). Only the agents giving differential responses in the siTop1 and siCtrl cells will be discussed here.

Both siTop1 cell lines were 6- to 8-fold resistant to camptothecin (Fig. 6 and Supplementary Table S3*A*) and to the indenoisoquinoline NSC 706744 (MJ-III-65; ref. 27), which both target Top1 directly (5). The siTop1 cell lines were also resistant to 4-NQO, which traps Top1cc as it forms carcinogenic DNA adducts (9). Both siTop1 cell lines showed slight resistance to the potent apoptosis inducer staurosporine (28), which may be attributable to the role of Top1 in promoting apoptosis (5, 29). Both siTop1 cell lines were also slightly resistant to aphidicolin and hydroxyurea, possibly as a result of a replication slowdown (see Fig. 3*C*). Chk1 activation by aphidicolin was also attenuated in HCT116 siTop1 cells (Supplementary Fig. S3*A*).

Conversely, both siTop1 cell lines were 2-fold hypersensitive to etoposide (Fig. 6), consistent with increased Top2α cleavage complexes (see Fig. 1*C* and *D*). The siTop1 cells were hypersensitive to L-asparaginase (Fig. 6), an observation consistent with ASNS down-regulation (see Top1 regulates ASNS expression). Both siTop1 cell lines were also hypersensitive to actinomycin D (Fig. 6), which may be related to the importance of Top1 for rDNA transcription.

Discussion

In this study, we designed and introduced Top1 siRNA constructs into human cell lines to establish siTop1 cell lines from two different tissues of origin (colon carcinoma HCT116-siTop1 and breast carcinomas MCF-7-siTop1). Both siTop1 cell lines show a stable ~5-fold reduction of Top1 expression.

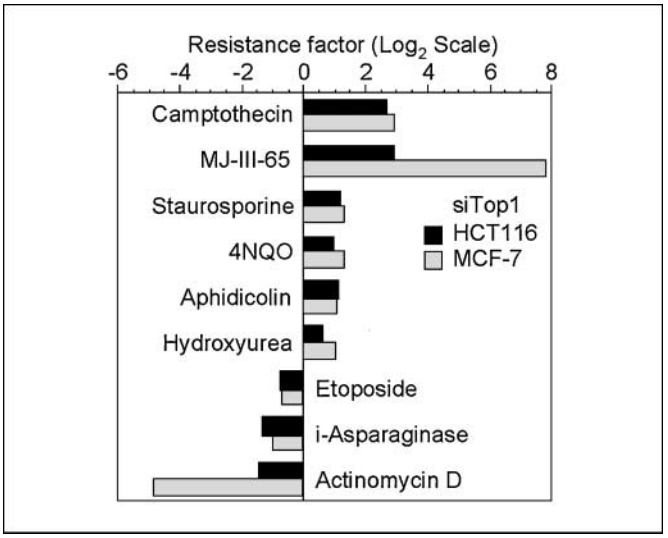

Figure 6. Differential sensitivity of the siTop1 cell lines to anticancer agents. Cells were treated with the indicated drugs for 72 h. Cell survival was measured by SRB assays. The resistance factor is the ratio of the IC_{50} value obtained from at least three independent experiments for the siTop1 cells to that of the corresponding siCtrl cells (see Supplementary Table S3 for mean IC_{50} values ±SD). Additional agents tested but giving no significant difference are not shown in the figure (see Supplementary Table S4).

However, neither of the siTop1 clones lacked Top1, consistent with the idea that, in contrast to yeast (2), human cells require Top1 [as do mouse and fly embryos (6, 7)]. The studies reported here provide the first direct lines of evidence for nonclassic roles of human Top1 in maintaining genomic stability, regulating gene-specific transcription and determining response to anticancer drugs.

Human Top1 and genomic integrity. Previous studies have shown that Top1 inhibitors can induce deletion mutations (30), chromosomal aberrations (31), and replication double-strand breaks (10). However, using Top1 inhibitors (e.g., CPT) cannot appropriately define the role of Top1 in genomic stability because drug-stabilized Top1cc act as DNA damage lesions. Our finding that both siTop1 cell lines exhibit genomic alterations in the absence of drug treatment (Figs. 2 and 3) indicate that Top1 deficiency in human cells leads to chromosomal rearrangements (Fig. 2*A*), replication slowdown and replication-associated DNA lesions (Fig. 3*A–C*), as well as rDNA (Fig. 2*B*) and nucleolar alterations (Fig. 3*D*).

Although yeast and human Top1s are relatively conserved (32), genetic and functional insights derived from yeast can be extrapolated to humans only with caution because genetic inactivation of Top1 is not lethal in either budding (33) or fission yeast (34), whereas knocking out the TOP1 gene is lethal in mice (7) and flies (6). The more stringent requirement for Top1 in human cells may be related to the complexity of the human genome, with its developmental and epigenetic controls. In agreement with the fact that Top1 is the major replication swivel in yeast (35), the human siTop1 cells showed replication defects, including replication-associated γ-H2AX foci (Fig. 3*A* and *B*), reduced nucleotide incorporation (Fig. 3*C*), and resistance to aphidicolin and hydroxyurea (Fig. 6 and Supplementary Table S3). Top1 deficiency may increase replication fork stalling and collapse because of excess superhelical tension in replicating chromatin domains (35).

The siTop1 cells are also characterized by abnormally high levels of chromosomal structure rearrangement (Fig. 2). Those rearrangements may arise from the replication defects discussed above and/or may be linked to chromatin alterations. Indeed, in *Xenopus* extracts, Top1 is the dominant actor in chromatin assembly (36). Our micrococcal nuclease analyses showed comparable nucleosomal patterns in siTop1 cells and their normal counterpart (Fig. 2*C*). Thus, chromatin perturbations resulting from Top1 deficiency may be localized to certain genomic regions and may not be detectable by global analyses. Consistently, in yeast, Top1 deficiency increases negative supercoiling without producing detectable changes in nucleosomal spacing (37). The increase in Top2α in both siTop1 cell lines might correspond to a compensatory mechanism for Top1 deficiency as Top2α has recently been shown to relax positive supercoiling preferentially, whereas Top2β and Top3 are equally effective at removing positive and negative supercoiling (38). However, the compensatory increase of Top2α activity might contribute, together with the Top1 deficiency, to the chromosomal rearrangements observed in the siTop1 cells because Top2 can promote chromosomal translocations (39).

Another characteristic of the siTop1 cells is the presence of structural alterations. Both siTop1 cell lines (particularly the MCF-7-siTop1 cells) showed increased numbers of nucleoli and heterogeneity in nucleolar size (Fig. 3*D*). Such nucleolar defects may be related to the nucleolar concentration of Top1 in normal

cells and the binding of Top1 to nucleolin (40), which is an important component of the nucleolus. Top1 deficiency also resulted in the lack of NOR staining on one of chromosomes 21 in HCT116-siTop1 cells, consistent with either the loss or reduction in size of rDNA cluster. Top1 deficiency in yeast also increases mitotic recombination in the rDNA cluster (24). An unexpected finding in the siTop1 cells was the apparent increase in nuclear size, especially in the MCF-7-siTop1 cells (Fig. 3*D*). That finding may be related to previous observations of nuclear abnormalities in TOP1-null yeast (34). Increased supercoiling has been proposed to alter the density of the corresponding chromatin regions because chromatin domains are anchored to the nuclear membrane (34). Thus, the examination of the siTop1 cells shows that human Top1 may regulate both chromatin structure and organization, as well as genomic stability.

Gene-specific transcriptional regulation by human Top1. Top1 regulates gene transcription in at least two ways. One is by way of the enzymatic activity of Top1, which relaxes DNA superhelical tension generated during transcription (1, 2, 5, 32); the other results from the coordination of Top1 with the activities of gene-specific transcriptional activators and general transcriptional factors, independently of Top1 catalytic activity (12–15). Prior studies on the regulation of transcription by Top1 were conducted in cellular systems focusing on specific genes (15, 41, 42). However, those observations did not address whether all genes or only some specific genes are under transcriptional regulation by Top1. Answering that question could be crucial to our understanding of the lethal phenotype of Top1 knock-out in mice and flies (6, 7) and possibly in human cells.

Profiling mRNA expression with spotted oligonucleotide microarrays showed 55 genes whose expression was altered in both siTop1 cell lines (Fig. 4). Considering that those genes are altered in both cell lines despite their different tissues of origin (i.e., breast and colon), we conclude the involvement of Top1 in the transcriptional regulation of at least some of those 55 genes. The complete data set will be made publicly available at the Discover Web site[11] and has been deposited in the Gene Expression Omnibus of the NCBI (GEO series accession number GSE7161).[9] Our current analysis did not focus on colon- or breast-specific differences. Nevertheless, Top1 has been implicated in tissue-specific transcriptional regulation, for example, in the case of the epidermal growth factor receptor (EGFR) gene, whose expression has been reported to be positively regulated by Top1 in human fibrosarcoma HT-1080 cells (15). However, we find EGFR gene expression to be within normal levels in our colon and breast carcinoma siTop1 cells. Comparison of our microarray gene list (Fig. 4*B* and Supplementary Table S1) from the siTop1 cell lines with those from camptothecin-treated human cell lines shows no similarity in gene expression changes. The dissimilarities probably reflect the fact that Top1 inhibitors primarily activate DNA damage responses (43) rather than simply reducing Top1 catalytic activity.

Only 4 of the 55 differentially expressed genes were up-regulated (Fig. 4 and Supplementary Table S1). Two of those genes belong to the group of nucleic acid and chromatin binding factors, HIST1H2BD (coding for histone H2B type 1-D) and NR2F2, which may compensate for the transcriptional defects resulting from Top1 down-regulation. The two other up-regulated genes, CD59 and GIP3, both encode factors that protect cells (44, 45). We also found the inactivation in the BAX gene in HCT116-siTop1 cells (data not shown). Thus, the inactivation of death pathways may provide a growth advantage to the siTop1 cells as they accumulate replication-associated DNA damage and genomic lesions.

ASNS is among the 51 genes consistently down-regulated in both siTop1 cell lines (Fig. 4). The fact that the genes immediately flanking the ASNS gene locus in chromosome 7 are not differentially expressed in the siTop1 cells (Fig. 4*C*) suggests a specific effect of Top1 on the ASNS gene, rather than a regional chromosomal effect. Moreover, the parallel expression of ASNS and Top1 mRNA and protein levels in response to the transient reduction of Top1 protein and to Top1 complementation (Fig. 5) suggests a direct causal relationship between Top1 and ASNS expression. Thus, it is likely that Top1 is specifically involved in the up-regulation of ASNS transcription. However, the reverse is not true; the down-regulation of ASNS by siRNA does not affect Top1 expression (Fig. 5*D*). ASNS is a housekeeping gene. Its main promoter contains no conventional TATA and CAAT boxes. It contains GC boxes (putative SP1 sites) and multiple transcription start sites and, notably, a nutrient-sensing response unit located within the ASNS main promoter (46, 47). In addition to ASNS, 11 metabolism genes (20% of all changed genes) were down-regulated in the siTop1 cells (Supplementary Table S1), suggesting that Top1 may be involved in the regulation of housekeeping genes. The mechanism of such regulation and, more specifically, the role of DNA supercoiling in the regulation of metabolism and transport genes deserve further study.

Roles of human Top1 in responses to anticancer agents and apoptosis. The siTop1 cell lines provided us with a way to test the effect of Top1 on cellular sensitivity to diverse anticancer agents. Staurosporine is a protein kinase inhibitor and a remarkably potent and widely used inducer of apoptosis in a variety of cell lines (28), which also induces apoptotic Top1cc (11). The resistance of both siTop1 cell lines to staurosporine (Fig. 6 and Supplementary Table S1*A*) provides functional evidence for a role of Top1 in apoptotic cell death.

The drugs showing increased activity in both Top1–down-regulated cell lines include L-asparaginase, etoposide (VP-16), and actinomycin D (Fig. 6; Supplementary Table S3*B*). Because ASNS expression is related to cellular resistance to L-ASP (Fig. 6) and because the reduction of Top1 levels is observed in cells treated with Top1 inhibitors (48), the results presented here open the novel possibility of combining L-ASP with a Top1 inhibitor for cancer treatment.

The pharmacologic experiments discussed above show the utility of the siTop1 cell lines as new tools for studying the role of Top1 as a target for not only therapeutic but also carcinogenic agents. That approach is complementary to the use of yeast cells lacking Top1 (4, 49), with the advantage of avoiding cell permeability limitations in yeast and of being closer to human tissues in the case of drugs with therapeutic potential.

Acknowledgments

Received 12/11/2006; revised 6/8/2007; accepted 6/28/2007.

Grant support: NIH, National Cancer Institute, Center for Cancer Research.

The costs of publication of this article were defrayed in part by the payment of page charges. This article must therefore be hereby marked *advertisement* in accordance with 18 U.S.C. Section 1734 solely to indicate this fact.

[11] http://discover.nci.nih.gov

References

1. Champoux JJ. DNA topoisomerases: structure, function, and mechanism. Annu Rev Biochem 2001;70:369–413.
2. Wang JC. Cellular roles of DNA topoisomerases: a molecular perspective. Nat Rev Mol Cell Biol 2002;3:430–40.
3. Hsiang YH, Hertzberg R, Hecht S, Liu LF. Camptothecin induces protein-linked DNA breaks via mammalian DNA topoisomerase I. J Biol Chem 1985;260:14873–8.
4. Nitiss J, Wang JC. DNA topoisomerase-targeting antitumor drugs can be studied in yeast. Proc Natl Acad Sci U S A 1988;85:7501–5.
5. Pommier Y. Topoisomerase I inhibitors: camptothecins and beyond. Nat Rev Cancer 2006;6:789–802.
6. Lee MP, Brown SD, Chen A, Hsieh TS. DNA topoisomerase I is essential in *Drosophila melanogaster*. Proc Natl Acad Sci U S A 1993;90:6656–60.
7. Morham SG, Kluckman KD, Voulomanos N, Smithies O. Targeted disruption of the mouse topoisomerase I gene by camptothecin selection. Mol Cell Biol 1996;16:6804–9.
8. Pommier Y, Barcelo JM, Rao VA, et al. Repair of topoisomerase I-mediated DNA damage. Prog Nucleic Acid Res Mol Biol 2006;81:179–229.
9. Miao ZH, Rao VA, Agama K, Antony S, Kohn KW, Pommier Y. 4-Nitroquinoline-1-oxide induces the formation of cellular topoisomerase I-DNA cleavage complexes. Cancer Res 2006;66:6540–5.
10. Furuta T, Takemura H, Liao ZY, et al. Phosphorylation of histone H2AX and activation of Mre11, Rad50, and Nbs1 in response to replication-dependent DNA-double-strand breaks induced by mammalian DNA topoisomerase I cleavage complexes. J Biol Chem 2003;278:20303–12.
11. Sordet O, Khan QA, Plo I, et al. Apoptotic topoisomerase I-DNA complexes induced by staurosporine-mediated oxygen radicals. J Biol Chem 2004;279:50499–504.
12. Merino A, Madden KR, Lane WS, Champoux JJ, Reinberg D. DNA topoisomerase I is involved in both repression and activation of transcription. Nature 1993;365:227–32.
13. Shykind BM, Kim J, Stewart L, Champoux JJ, Sharp PA. Topoisomerase I enhances TFIID-TFIIA complex assembly during activation of transcription. Genes Dev 1997;11:397–407.
14. Kretzschmar M, Meisterernst M, Roeder RG. Identification of human DNA topoisomerase I as a cofactor for activator-dependent transcription by RNA polymerase II. Proc Natl Acad Sci U S A 1993;90:11508–12.
15. Mialon A, Sankinen M, Soderstrom H, et al. DNA topoisomerase I is a cofactor for c-Jun in the regulation of epidermal growth factor receptor expression and cancer cell proliferation. Mol Cell Biol 2005;25:5040–51.
16. Soret J, Gabut M, Dupon C, et al. Altered serine/arginine-rich protein phosphorylation and exonic enhancer-dependent splicing in mammalian cells lacking topoisomerase I. Cancer Res 2003;63:8203–11.
17. Takebayashi Y, Pourquier P, Zimonjic DB, et al. Antiproliferative activity of ecteinascidin 743 is dependent upon transcription-coupled nucleotide-excision repair. Nat Med 2001;7:961–6.
18. Howell WM, Black DA. Controlled silver-staining of nucleolus organizer regions with a protective colloidal developer: a 1-step method. Experientia 1980;36:1014–5.
19. Subramanian D, Furbee CS, Muller MT. ICE bioassay. Isolating *in vivo* complexes of enzyme to DNA. Methods Mol Biol 2001;95:137–47.
20. Sordet O, Liao Z, Liu H, et al. Topoisomerase I–DNA complexes contribute to arsenic trioxide-induced apoptosis. J Biol Chem 2004;279:33968–75.
21. Whang-Peng J, Lee EC, Kao-Shan CS, Seibert K, Lippman M. Cytogenetic studies of human breast cancer lines: MCF-7 and derived variant sublines. J Natl Cancer Inst 1983;71:687–95.
22. Jones C, Payne J, Wells D, Delhanty JD, Lakhani SR, Kortenkamp A. Comparative genomic hybridization reveals extensive variation among different MCF-7 cell stocks. Cancer Genet Cytogenet 2000;117:153–8.
23. Lengauer C, Kinzler KW, Vogelstein B. Genetic instability in colorectal cancers. Nature 1997;386:623–7.
24. Christman MF, Dietrich FS, Fink GR. Mitotic recombination in the rDNA of *S. cerevisiae* is suppressed by the combined action of DNA topoisomerases I and II. Cell 1988;55:413–25.
25. Pilch DR, Sedelnikova OA, Redon C, Celeste A, Nussenzweig A, Bonner WM. Characteristics of γ-H2AX foci at DNA double-strand breaks sites. Biochem Cell Biol 2003;81:123–9.
26. Gorgoulis VG, Vassiliou LV, Karakaidos P, et al. Activation of the DNA damage checkpoint and genomic instability in human precancerous lesions. Nature 2005;434:907–13.
27. Antony S, Kohlhagen G, Agama K, et al. Cellular Topoisomerase I inhibition and antiproliferative activity by MJ-III-65 (NSC 706744), an indenoisoquinoline topoisomerase I poison. Mol Pharmacol 2005;67:523–30.
28. Bertrand R, Solary E, Kohn KW, O'Connor P, Pommier Y. Induction of a common pathway to apoptosis by staurosporine. Exp Cell Res 1994;211:314–21.
29. Sordet O, Khan QA, Pommier Y. Apoptotic topoisomerase I–DNA complexes induced by oxygen radicals and mitochondrial dysfunction. Cell Cycle 2004;3:1095–7.
30. Balestrieri E, Zanier R, Degrassi F. Molecular characterisation of camptothecin-induced mutations at the HPRT locus in Chinese hamster cells. Mutat Res 2001;476:63–9.
31. Degrassi F, De Salvia R, Tanzarella C, Palitti F. Induction of chromosomal aberrations and SCE by camptothecin, an inhibitor of mammalian topoisomerase I. Mutat Res 1989;211:125–30.
32. Gupta M, Fujimori A, Pommier Y. Eukaryotic DNA topoisomerases I. Biochim Biophys Acta 1995;1262:1–14.
33. Thrash C, Voelkel K, DiNardo S, Sternglanz R. Identification of *Saccharomyces cerevisiae* mutants deficient in DNA topoisomerase I activity. J Biol Chem 1984;259:1375–7.
34. Uemura T, Yanagida M. Isolation of type I and II DNA topoisomerase mutants from fission yeast: single and double mutants show different phenotypes in cell growth and chromatin organization. EMBO J 1984;3:1737–44.
35. Kim RA, Wang JC. Function of DNA topoisomerases as replication swivels in *Saccharomyces cerevisiae*. J Mol Biol 1989;208:257–67.
36. Almouzni G, Mechali M. Assembly of spaced chromatin involvement of ATP and DNA topoisomerase activity. EMBO J 1988;7:4355–65.
37. Cavalli G, Bachmann D, Thoma F. Inactivation of topoisomerases affects transcription-dependent chromatin transitions in rDNA but not in a gene transcribed by RNA polymerase II. EMBO J 1996;15:590–7.
38. McClendon AK, Dickey JS, Osheroff N. Ability of viral topoisomerase II to discern the handedness of supercoiled DNA: bimodal recognition of DNA geometry by type II enzymes. Biochemistry 2006;45:11674–80.
39. Felix CA, Kolaris CP, Osheroff N. Topoisomerase II and the etiology of chromosomal translocations. DNA Repair (Amst) 2006;5:1093–108.
40. Edwards TK, Saleem A, Shaman JA, et al. Role for nucleolin/Nsr1 in the cellular localization of topoisomerase I. J Biol Chem 2000;275:36181–8.
41. Stewart AF, Herrera RE, Nordheim A. Rapid induction of c-fos transcription reveals quantitative linkage of RNA polymerase II and DNA topoisomerase I enzyme activities. Cell 1990;60:141–9.
42. Li CJ, Wang C, Pardee AB. Camptothecin inhibits Tat-mediated transactivation of type 1 human immunodeficiency virus. J Biol Chem 1994;269:7051–4.
43. Daoud SS, Munson PJ, Reinhold W, et al. Impact of p53 knockout and topotecan treatment on gene expression profiles in human colon carcinoma cells: a pharmacogenomic study. Cancer Res 2003;63:2782–93.
44. Qin X, Ferris S, Hu W, Guo F, Ziegeler G, Halperin JA. Analysis of the promoters and 5′-UTR of mouse Cd59 genes, and of their functional activity in erythrocytes. Genes Immun 2006;7:287–97.
45. Tahara E, Jr., Tahara H, Kanno M, et al. G1P3, an interferon inducible gene 6–16, is expressed in gastric cancers and inhibits mitochondrial-mediated apoptosis in gastric cancer cell line TMK-1 cell. Cancer Immunol Immunother 2005;54:729–40.
46. Zhong C, Chen C, Kilberg MS. Characterization of the nutrient-sensing response unit in the human asparagine synthetase promoter. Biochem J 2003;372:603–9.
47. Guerrini L, Gong SS, Mangasarian K, Basilico C. Cis- and trans-acting elements involved in amino acid regulation of asparagine synthetase gene expression. Mol Cell Biol 1993;13:3202–12.
48. Beidler DR, Cheng Y-C. Camptothecin induction of a time- and concentration-dependent decrease of topoisomerase I and its implication in camptothecin activity. Mol Pharmacol 1995;47:907–14.
49. Bjornsti M-A, Benedetti P, Viglianti GA, Wang JC. Expression of human DNA topoisomerase I in yeast cells lacking yeast DNA topoisomerase I: restoration of sensitivity of the cells to the antitumor drug camptothecin. Cancer Res 1989;49:6318–23.

Nonclassic Functions of Human Topoisomerase I: Genome-Wide and Pharmacologic Analyses

Ze-Hong Miao, Audrey Player, Uma Shankavaram, et al.

Cancer Res 2007;67:8752-8761.